VBF Higgs production in the structure function approach and beyond

Alexander Karlberg (University of Zurich)

Future challenges for precision QCD 25 October 2016

Based on PRL115(082002) and PRL117(072001) in collaboration with

Matteo Cacciari, Frédéric Dreyer, Gavin Salam & Giulia Zanderighi.

This work

- first semi-differential N^{3}LO calculation of VBF Higgs production in the structure function approach
- first fully differential NNLO calculation of VBF Higgs production using a novel "projection-to-Born" method

What to expect

- N^{3}LO corrections are at the permille level and well within the scale uncertainty band of the NNLO prediction
- the associated scale uncertainty is reduced by a factor 5 at N^{3}LO
- NNLO corrections are sizeable, $\mathcal{O}(10\%)$, and outside NLO band
- the corrections are (almost everywhere) negative
- only moderate shrinkage of NNLO bands compared to NLO bands
- the "projection-to-Born" method is quite general and can be extended to other similar processes

Reasons to study VBF

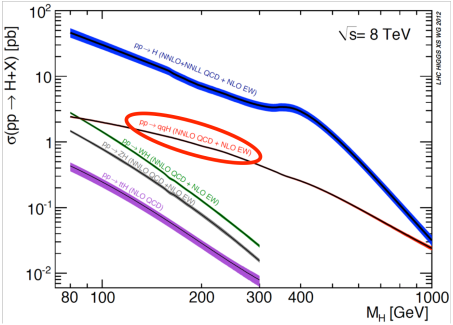

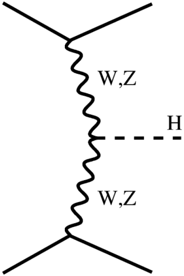

- largest cross section at tree-level and second-largest of all channels
- distinct signature of two forward jets
- tagging reduces backgrounds (eg $H \to b\bar{b}$)
- non-zero Higgs transverse momentum at lowest order
- sensitive to CP properties of the Higgs through correlation of forward jets
- sensitive to trilinear Higgs self-coupling through loop-corrections

Reasons to study VBF

Production process	ATLAS+CMS	ATLAS	CMS
μ_{ggF}	$1.03^{+0.17}_{-0.15}$	$1.25^{+0.24}_{-0.21}$	$0.84^{+0.19}_{-0.16}$
μ_{VBF}	$1.18^{+0.25}_{-0.23}$	$1.21^{+0.33}_{-0.30}$	$1.13^{+0.37}_{-0.34}$
μ_{WH}	$0.88^{+0.40}_{-0.38}$	$1.25^{+0.56}_{-0.52}$	$0.46^{+0.57}_{-0.54}$
μ_{ZH}	$0.80^{+0.39}_{-0.36}$	$0.30^{+0.51}_{-0.46}$	$1.35^{+0.58}_{-0.54}$
μ_{ttH}	$2.3^{+0.7}_{-0.6}$	$1.9^{+0.8}_{-0.7}$	$2.9^{+1.0}_{-0.9}$

- largest cross section at tree-level and second-largest of all channels
- distinct signature of two forward jets
- tagging reduces backgrounds (eg $H \to b\bar{b}$)
- non-zero Higgs transverse momentum at lowest order
- sensitive to CP properties of the Higgs through correlation of forward jets
- sensitive to trilinear Higgs self-coupling through loop-corrections

Inclusive NNLO VBF Higgs Production

Until recently VBF Higgs production was only known inclusively at NNLO. [Bolzoni et al. (2010)]

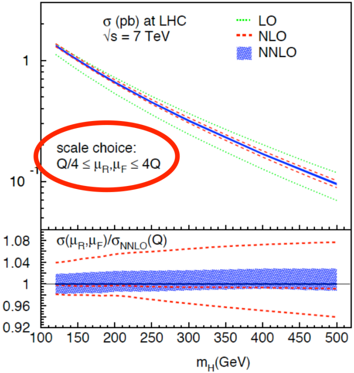

- the calculation suggests tiny renormlisation and factorisation scale variations $(\sim 1-2\%)$
- NNLO results well within NLO band
- result obtained in the structure function approach

No cuts can be applied to the calculation, as it is totally inclusive over hadronic final states with the same vector boson momenta.

Exclusive NLO VBF Higgs Production

To enable the application of realistic VBF cuts one has to be fully differential. Until recently differential VBF Higgs production was known to NLO(+PS). [Figy, Oleari, Zeppenfeld (2003)]

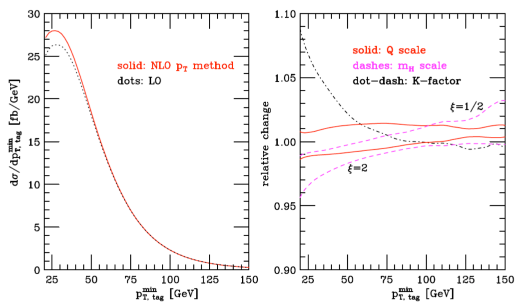

Calculation suggests small uncertainties from missing higher order corrections ($\sim 2\%$).

Structure Function Approach

One can think of VBF Higgs production as a double Deep Inelastic Scattering (DIS×DIS) with no cross-talk between the upper and lower sectors.

[Han, Valencia, Willenbrock (1992)]

- this picture is accurate to more than 1%

[Bolzoni et al. (2012)], [Ciccolini, Denner, Dittmaier (2008)], [Harlander et al. (2008)], [Andersen et al. (2008)]

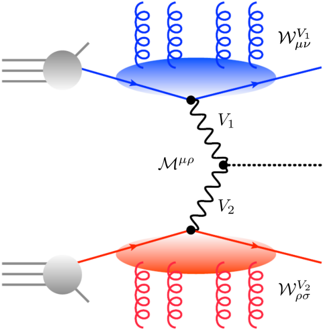

- the factorisation of the two sectors is exact if one imagines two copies of QCD, QCD_1 and QCD_2 , respectively for the upper and lower sectors.
- all DIS coefficients are known to to $\mathrm{N^3LO}$.
- as the DIS coefficients are inclusive over the hadronic final state, the calculation cannot provide differential results.

Structure Function Approach

$$d\sigma_{\mathrm{VBF}} = \frac{G_F^2}{s} M_{V_1}^2 M_{V_2}^2 \Delta_{V_1}^2(Q_1^2)\Delta_{V_2}^2(Q_2^2) \times$$
$$\mathcal{W}_{\mu\nu}^{V_1}(x_1, Q_1^2)\mathcal{M}^{\mu\rho}\mathcal{M}^{*\nu\sigma}\mathcal{W}_{\rho\sigma}^{V_2}(x_2, Q_2^2)\, d\Omega_{\mathrm{VBF}}$$

and

$$\mathcal{M}^{\mu\nu} = 2\sqrt{\sqrt{2}G_F} M_V^2 g^{\mu\nu}$$

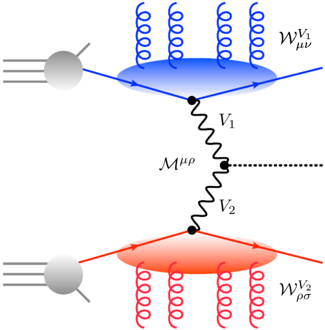

Hadronic Tensor

$$\mathcal{W}_{\mu\nu}^{V}(x_i, Q_i^2) =$$
$$\left(-g_{\mu\nu} + \frac{q_{i,\mu}q_{i,\nu}}{q_i^2}\right) F_1^V(x_i, Q_i^2)$$
$$+ \frac{\hat{P}_{i,\mu}\hat{P}_{i,\nu}}{P_i \cdot q_i} F_2^V(x_i, Q_i^2)$$
$$+ i\epsilon_{\mu\nu\rho\sigma}\frac{P_i^\rho q_i^\sigma}{2P_i \cdot q_i} F_3^V(x_i, Q_i^2)$$

Structure Function Approach

The Structure Functions can be expressed as convolutions of the short distance DIS coefficient functions and PDFs

$$F_i^V = \sum_{a=q,g} C_{i,a}^V \otimes f_a \,, \quad i = 2, L, 3 \,, \quad V = Z, W^+, W^- \,,$$

where DIS coefficient functions are known to the third order in α_s. [Moch, Rogal, Vermaseren, Vogt (2005-2008)]

Conceptually N^{3}LO not more complicated than NNLO, but non-trivial flavour structures start appearing at N^{3}LO

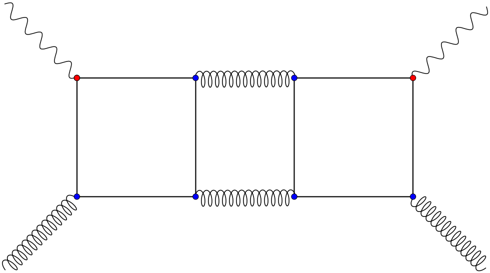

What about missing N^{3}LO PDFs?

All approximations aside, we can't truely claim N^{3}LO accuracy without also having N^{3}LO PDFs available.
Naive estimate

$$\delta_A^{\text{PDF}} = \frac{1}{2}\left|\frac{\sigma^{\text{NNLO}}_{\text{NNLO-PDF}} - \sigma^{\text{NNLO}}_{\text{NLO-PDF}}}{\sigma^{\text{NNLO}}_{\text{NNLO-PDF}}}\right| = 1.1\%\,,$$

and slightly more sophisticated ($Q_0 = 8$ GeV)

$$f^{\text{N}^3\text{LO,approx.}}(x,Q) = f^{\text{NNLO}}(x,Q)\,\frac{F_2^{\text{NNLO}}(x,Q_0)}{F_2^{\text{N}^3\text{LO}}(x,Q_0)}\,,$$

$$\delta_B^{\text{PDF}}(Q_0) = \left|\frac{\sigma^{\text{N}^3\text{LO}} - \sigma^{\text{N}^3\text{LO}}_{\text{rescaled}}(Q_0)}{\sigma^{\text{N}^3\text{LO}}}\right| = 7.9‰\,.$$

What about missing N^{3}LO PDFs?

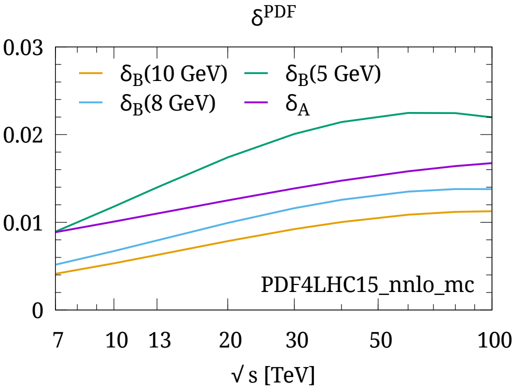

- the value of $Q_0 = 8\,\text{GeV}$ is found by requiring that the method is reliable in estimating NNLO corrections to PDFs
- the uncertainty associated with varying the scale in the DGLAP evolutions is found to be below the permille level

$\rightarrow$ could obtain approximate N^{3}LO PDFs using just N^{3}LO coefficient functions

Scale variations at N^{3}LO

We use RGE methods to evaluate the structure functions at arbitrary renormalisation scales

$$\alpha_S(Q) = \alpha_S(\mu_R) + \alpha_S^2(\mu_R)\beta_0 L_{RQ} + \alpha_S^3(\mu_R)(\beta_0^2 L_{RQ}^2 + \beta_1 L_{RQ}) + \mathcal{O}(\alpha_S^4(\mu_R))$$

$$L_{RQ} = \ln\left(\frac{\mu_R{}^2}{Q^2}\right), \quad L_{FQ} = \ln\left(\frac{\mu_F{}^2}{Q^2}\right)$$

$$C_i = \sum_{k=0}\left(\frac{\alpha_S(Q)}{2\pi}\right)^k C_i^{(k)} =
C_i^{(0)} + \frac{\alpha_S(\mu_R)}{2\pi} C_i^{(1)} +
\left(\frac{\alpha_S(\mu_R)}{2\pi}\right)^2 \left(C_i^{(2)} + 2\pi\beta_0 C_i^{(1)} L_{RQ}\right) +
\left(\frac{\alpha_S(\mu_R)}{2\pi}\right)^3 \left[C_i^{(3)} + 4\pi\beta_0 C_i^{(2)} L_{RQ}
+ 4\pi^2 C_i^{(1)} L_{RQ}(\beta_1 + \beta_0^2 L_{RQ})\right] + \mathcal{O}(\alpha_S^4)$$

$$f(x,Q) = f(x,\mu_F)\Bigg(1 - \frac{\alpha_S(\mu_R)}{2\pi} L_{FQ} P^{(0)}
- \left(\frac{\alpha_S(\mu_R)}{2\pi}\right)^2 L_{FQ}\Big[P^{(1)} - \frac{1}{2} L_{FQ}(P^{(0)})^2
- \pi\beta_0 P^{(0)}(L_{FQ} - 2L_{RQ})\Big]
- \left(\frac{\alpha_S(\mu_R)}{2\pi}\right)^3 L_{FQ}\Big[P^{(2)} - \frac{1}{2} L_{FQ}(P^{(0)}P^{(1)}
+ P^{(1)}P^{(0)}) + \pi\beta_0(L_{FQ} - 2L_{RQ})\times
(L_{FQ}(P^{(0)})^2 - 2P^{(1)}) + \frac{1}{6} L_{FQ}^2 (P^{(0)})^3
+ 4\pi^2\beta_0^2 P^{(0)}(L_{RQ}^2 - L_{FQ}L_{RQ} + \frac{1}{3} L_{FQ}^2)
- 2\pi^2\beta_1 P^{(0)}(L_{FQ} - 2L_{RQ})\Big] + \mathcal{O}(\alpha_S^4)\Bigg)$$

N^{3}LO results

	$\sigma^{(13\text{ TeV})}$ [pb]	$\sigma^{(14\text{ TeV})}$ [pb]	$\sigma^{(100\text{ TeV})}$ [pb]
LO	$4.099^{+0.051}_{-0.067}$	$4.647^{+0.037}_{-0.058}$	$77.17^{+6.45}_{-7.29}$
NLO	$3.970^{+0.025}_{-0.023}$	$4.497^{+0.032}_{-0.027}$	$73.90^{+1.73}_{-1.94}$
NNLO	$3.932^{+0.015}_{-0.010}$	$4.452^{+0.018}_{-0.012}$	$72.44^{+0.53}_{-0.40}$
N^{3}LO	$3.928^{+0.005}_{-0.001}$	$4.448^{+0.006}_{-0.001}$	$72.34^{+0.11}_{-0.02}$

- We study pp collisions with PDF4LHC_nnlo_mc and electroweak parameters fixed to their PDG values
- the central renormalisation and factorisation scale is set equal to Q_1, Q_2 and varied independently by a factor 2 up and down
- N^{3}LO corrections are tiny $(\sim 2‰)$ but predictions well within NNLO scale uncertainty

N^{3}LO results

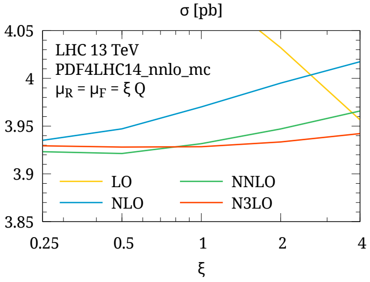

- the N^{3}LO corrections are tiny over a large range of energies and stay well within the scale uncertainty band of the NNLO prediction
- cross section becomes extremely stable under the variation of renormalisation and factorisation scales

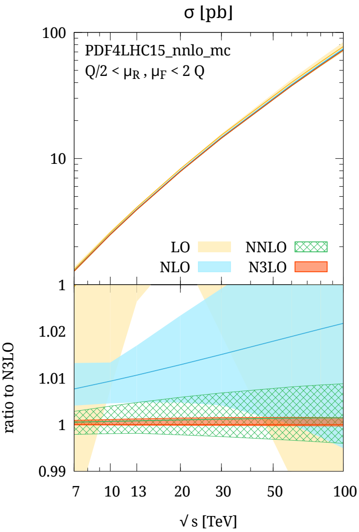

N^3LO results

From the knowledge of Q_1 and Q_2 it is trivial to reconstruct the momentum of the Higgs. The calculation is therefore fully differential in the Higgs kinematics.

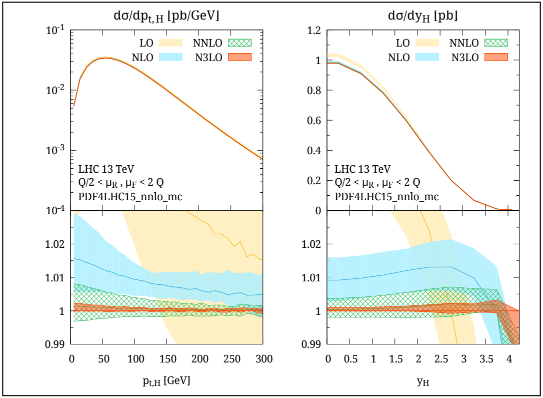

- the corrections are almost flat throughout the entire spectrum
- the N^3LO prediction completely contained within the scale uncertainty band of the NNLO prediction
- only differential in the momenta of the proton remnants, and hence no real information on the tagging jets

Limitations of the structure function approach

- gluon exchanges between the upper and lower hadronic sectors, which appear at NNLO, but are kinematically and colour suppressed; These contributions along with the heavy-quark loop induced contributions have been estimated to contribute at the permille level [Bolzoni et al. (2012)]
- t-/u-channel interference which are known to contribute $\mathcal{O}(5‰)$ at the fully inclusive level and $\mathcal{O}(0.5‰)$ after VBF cuts have been applied [Ciccolini, Denner, Dittmaier (2008)]
- contributions from s-channel production, which have been calculated up to NLO. At the inclusive level these contributions are sizeable but they are reduced to $\mathcal{O}(5‰)$ after VBF cuts [Ciccolini, Denner, Dittmaier (2008)]
- single-quark line contributions, which contribute to the VBF cross section at NNLO. At the fully inclusive level these amount to corrections of $\mathcal{O}(1\%)$ but are reduced to the permille level after VBF cuts have been applied [Harlander et al. (2008)]
- loop induced interference between VBF and ggH production. These contributions have been shown to be much below the permille level [Andersen et al. (2008)]

Beyond the Structure Function Approach

This work: We eliminate the limitations of the Structure Function Approach.

If the scattering is Born like, then the vector boson momenta q_i, and on-shell conditions, fix the incoming and outgoing parton momenta:

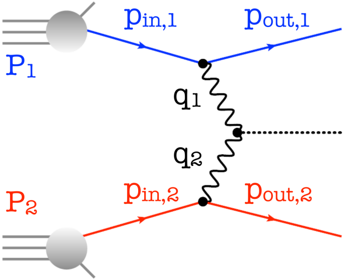

$$p_{in,i} = x_i P_i$$

$$p_{out,i} = x_i P_i - q_i$$

$$x_i = \frac{q_i^2}{2 q_i P_i}$$

Beyond the Structure Function Approach

The calculation is based on two ingredients:

1. *An "inclusive" contribution*
   - use the Structure Function Approach and use four-vectors q_1, q_2 to assign Born-like kinematics using the equations below
   - use the projected Born-like momenta to compute differential distributions

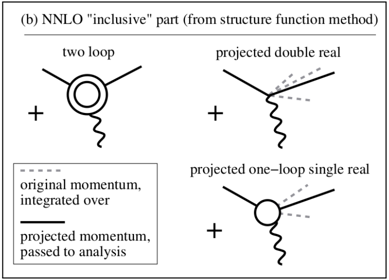

$$p_{in,i} = x_i P_i$$

$$p_{out,i} = x_i P_i - q_i$$

$$x_i = \frac{q_i^2}{2 q_i P_i}$$

Beyond the Structure Function Approach

The calculation is based on two ingredients:

2. *An "exclusive" contribution*
   - use the electroweak H+jjj NLO calculation in the factorized approximation [Figy et al. (2007)], [Jäger et al. (2014)]

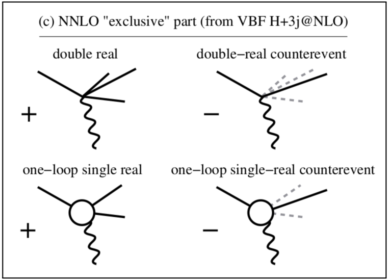

- for each parton, keep track of whether it belongs to the upper or lower sector, and compute vector-boson momenta
- for each event add counter-event with projected Born kinematics and opposite weight

The counter-events cancel identically with the projected terms from the "inclusive" contribution.

Beyond the Structure Function Approach

Schematically we express the "projection-to-Born" (P2B) method as

$$
\begin{aligned}
d\sigma &= \int d\Phi_B (B+V) + \int d\Phi_R R \\
&= \underbrace{\int d\Phi_B (B+V) + \int d\Phi_R R_{P2B}}_{\text{“inclusive” contribution}} + \underbrace{\int d\Phi_R R - \int d\Phi_R R_{P2B}}_{\text{“exclusive” contribution}}
\end{aligned}
$$

- from the "exclusive" ingredient we get the full double-real and one-loop single-real contributions.
- when integrated over phase-space, the counter-events cancel the projected double-real and one-loop single-real contributions from the "inclusive" ingredient

Hence the sum of the two contributions gives the complete, fully differential NNLO result.

Beyond the Structure Function Approach

Schematically we express the "projection-to-Born" (P2B) method as

$$\begin{aligned} d\sigma &= \int d\Phi_B (B+V) + \int d\Phi_R R \\ &= \underbrace{\int d\Phi_B (B+V) + \int d\Phi_R R_{P2B}}_{\text{“inclusive” contribution}} + \underbrace{\int d\Phi_R R - \int d\Phi_R R_{P2B}}_{\text{“exclusive” contribution}} \end{aligned}$$

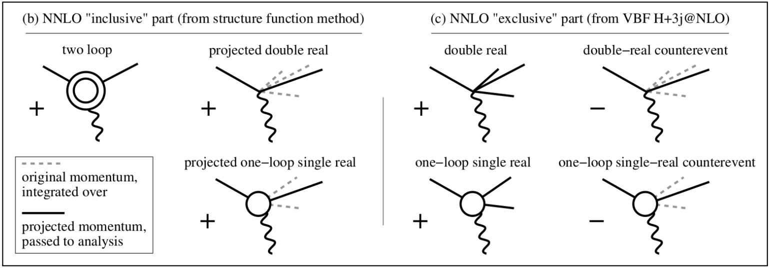

Implementation

1. "inclusive" code
    - matrix elements coded with structure functions using parametrised versions of the DIS coefficient functions evaluated by HOPPET
    - phase-space taken from POWHEG's VBF_H generator
2. "exclusive" code
    - start with the VBF_HJJJ calculation in POWHEG (based on vbfnlo)
    - extend POWHEG's tags to uniquely associate radiation with each sector (upper or lower line)
    - for each event map the kinematics onto Born-like kinematics and determine the vector-boson momenta q_1, q_2 using the equations on p.7.

- we have tested the "inclusive" code against a private version of the structure function calculation (thanks to Marco Zaro) and the structure functions themselves against APFEL 2.4.1.
- we have tested that the "exclusive" code reproduces the original VBF_HJJJ result. The sum of "inclusive" and "exclusive" at NLO agrees with VBF_H
- tagging tested by checking that the probablity of assigning a parton to the wrong sector decreases as the rapidity between the two hardest jets increases

Phenomenology

We study 13 TeV LHC collisions with $M_H = 125$ GeV and NNPDF3.0_nnlo_as118. We use the following VBF cuts:

- Jets defined with anti-k_t, $R = 0.4$ and $p_t > 25$ GeV
- Two hardest jets within $|y| < 4.5$
- High dijet invariant mass, $M_{j_1 j_2} > 600$ GeV, and separation, $\Delta y_{j_1 j_2} > 4.5$
- Hardest jets in opposite hemispheres, $y_{j_1} y_{j_2} < 0$

We choose a central scale which approximates well $\sqrt{Q_1 Q_2}$ and symmetrically vary by a factor 2 up and down

$$\mu_0^2(p_{t,H}) = \frac{M_H}{2}\sqrt{\left(\frac{M_H}{2}\right)^2 + p_{t,H}^2}$$

Phenomenology

	$\sigma^{\text{(no cuts)}}$ [pb]	$\sigma^{\text{(VBF cuts)}}$ [pb]
LO	$4.032^{+0.057}_{-0.069}$	$0.957^{+0.066}_{-0.059}$
NLO	$3.929^{+0.024}_{-0.023}$	$0.876^{+0.008}_{-0.018}$
NNLO	$3.888^{+0.016}_{-0.012}$	$0.826^{+0.013}_{-0.014}$

- NNLO corrections tiny ($\sim 1\%$) without cuts and sizeable with VBF cuts ($\sim 5\%$)
- NNLO results outside NLO band (also true when using NLO PDFs)
- corrections tend to be dominated by the extra real radiation. The effect is softer jets and hence fewer events pass the cuts

Phenomenology

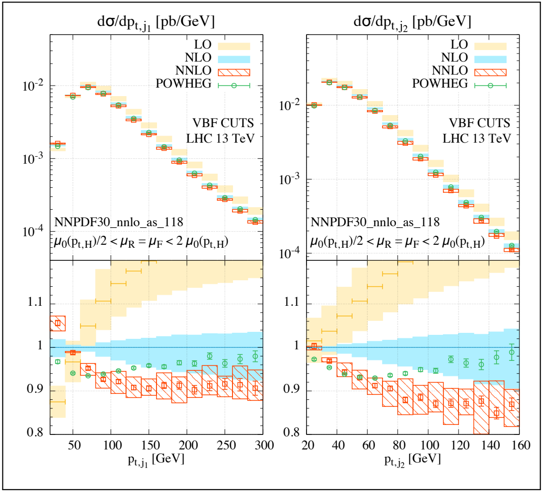

- NNLO corrections can be large $\mathcal{O}(10\%)$ and are often outside the NLO band
- the NNLO corrections tend to be dominated by extra real radiation. These appear to make the jets softer
- NOTE: NNLO PDF used everywhere. Similar results hold when using LO/NLO PDFs
- expanding the scale variation from 3-point to 7-point doesn't change the size of the NLO bands noticeably

More Phenomenology

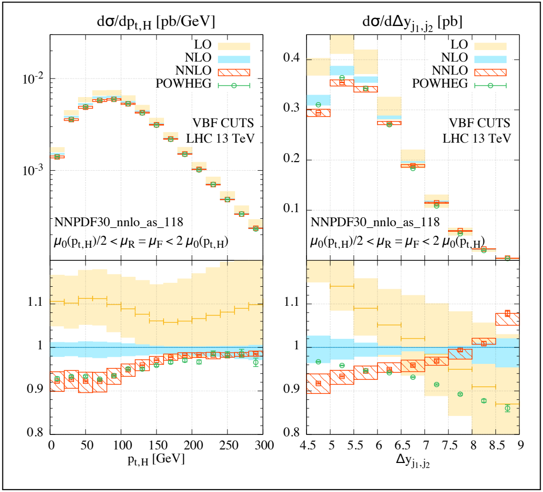

- in some cases NLO+PS agrees very well with the NNLO result (in particular $p_{t,H}$, M_{jj} and ϕ_{jj})
- in some cases not ($\Delta y_{j_1,j_2}$ and H_t)
- in general only modest shrinkage of bands from NLO to NNLO
- non-trivial kinematic dependence on k-factors (both LO/NLO and NNLO/NLO)

LHCHXWG YR4 results

We study LHC collisions with $M_H = 125$ GeV and PDF4LHC15_nnlo_100. We use the following setup:

- Jets defined with anti-k_t, $R = 0.4$ and $p_t > 20$ GeV
- Two hardest jets within $|y| < 5$
- Dijet invariant mass, $M_{j_1 j_2} > 130$ GeV, and separation, $\Delta y_{j_1 j_2} > 3$
- $\mu_R = \mu_F = M_W$ (varied a factor 2 up and down)
- Electroweak corrections obtained with HAWK [Ciccolini, Denner, Dittmaier (2008)]
- Photon PDF obtained from NNPDF2.3QED
- $\sigma^{\text{VBF}} = \sigma^{\text{DIS}}_{\text{NNLOQCD}}(1 + \delta_{\text{EW}}) + \sigma_\gamma$

$\sqrt{s}$[TeV]	σ^{VBF}[fb]	Δ_{scale}[%]	$\Delta_{\text{PDF}/\alpha_s/\text{PDF}\oplus\alpha_s}$[%]	$\sigma^{\text{DIS}}_{\text{NNLOQCD}}$[fb]	δ_{EW}[%]	σ_γ[fb]	$\sigma_{\text{s-channel}}$[fb]
7	1241	$^{+0.19}_{-0.21}$	$\pm 2.1/\pm 0.4/\pm 2.2$	1281	-4.4	17.1	584.5(3)
8	1601	$^{+0.25}_{-0.24}$	$\pm 2.1/\pm 0.4/\pm 2.2$	1656	-4.6	22.1	710.4(3)
13	3782	$^{+0.43}_{-0.33}$	$\pm 2.1/\pm 0.5/\pm 2.1$	3939	-5.3	51.9	1378.1(6)
14	4278	$^{+0.45}_{-0.34}$	$\pm 2.1/\pm 0.5/\pm 2.1$	4461	-5.4	58.5	1515.9(6)

$\sqrt{s}$[TeV]	σ^{VBF}[fb]	Δ_{scale}[%]	$\Delta_{\text{PDF}/\alpha_s/\text{PDF}\oplus\alpha_s}$[%]	$\sigma^{\text{DIS}}_{\text{NNLOQCD}}$[fb]	δ_{EW}[%]	σ_γ[fb]	$\sigma_{\text{s-channel}}$[fb]
7	602.4(5)	$^{+1.3}_{-1.6}$	$\pm 2.3/\pm 0.3/\pm 2.3$	630.8(5)	-6.1	9.9	8.2
8	795.9(6)	$^{+1.3}_{-1.5}$	$\pm 2.3/\pm 0.3/\pm 2.3$	834.8(7)	-6.2	13.1	11.1
13	1975(1)	$^{+1.3}_{-1.2}$	$\pm 2.1/\pm 0.4/\pm 2.2$	2084(1)	-6.8	32.3	29.0
14	2236(3)	$^{+1.5}_{-1.3}$	$\pm 2.1/\pm 0.4/\pm 2.1$	2362(3)	-6.9	36.7	33.1

LHCHXSWG YR4 results

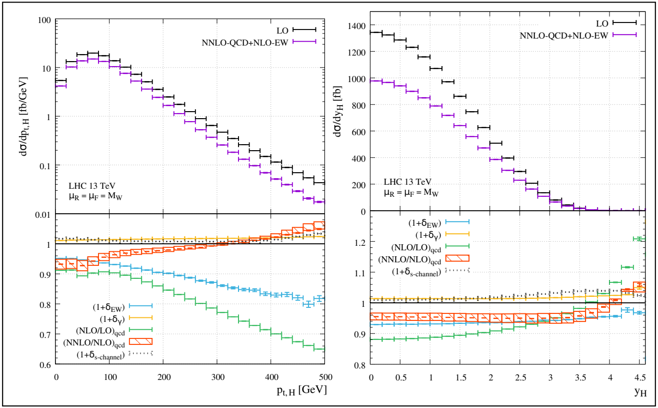

- NLO-QCD corrections can be very large (notice scale choice)
- NLO-EW corrections can be sizeable in the tails of distributions
- NNLO-QCD corrections of the same order as NLO-EW corrections
- Photon induced contribution very flat

LHCHXSWG YR4 results

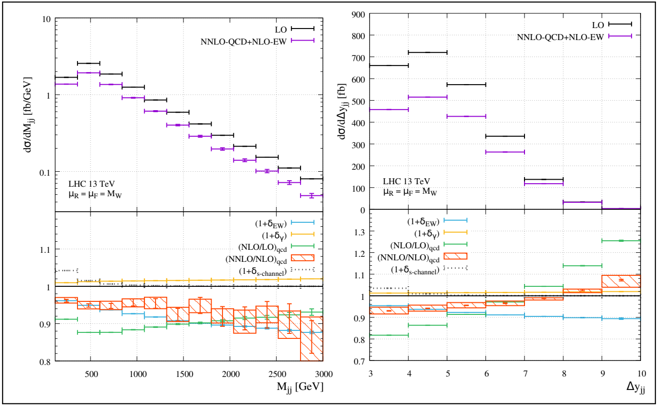

- NLO-QCD corrections can be very large (notice scale choice)
- NLO-EW corrections can be sizeable in the tails of distributions
- NNLO-QCD corrections of the same order as NLO-EW corrections
- Photon induced contribution very flat

Conclusions

- inclusive N^3LO are tiny and well within scale uncertainty band at NNLO
- scale uncertainty band reduced significantly
- differential NNLO corrections are sizeable, $\mathcal{O}(10\%)$, and necessary for precision phenomenology
- only moderate shrinkage of NNLO bands compared to NLO bands
- NLO-EW corrections are comparable to NNLO-QCD corrections and should be included
- "projection-to-Born" method can be extended to compute fully differential VBF Higgs at N^3LO

A public code, `proVBFH`, will be released in the near future. Until then total cross sections and distributions with specific cuts can be provided.

Tagging

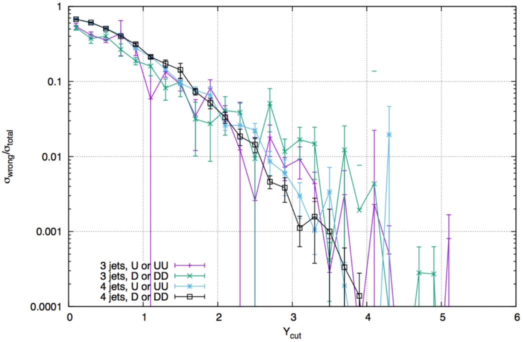

With no bug in the code, the probability of a tagged parton having wrong rapidity decreases with increasing rapidity separation between the two hardest jets.

Tagging

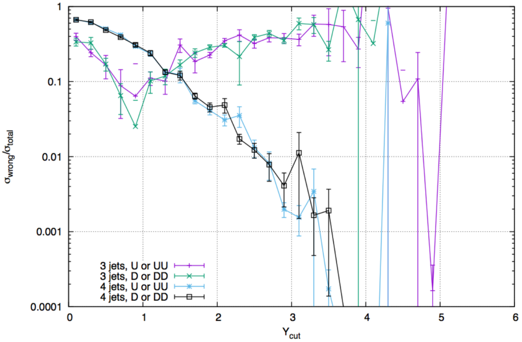

With an $\mathcal{O}(1)$ bug in the code, this is clearly not the case any more.

3-point vs 7-point scale variations

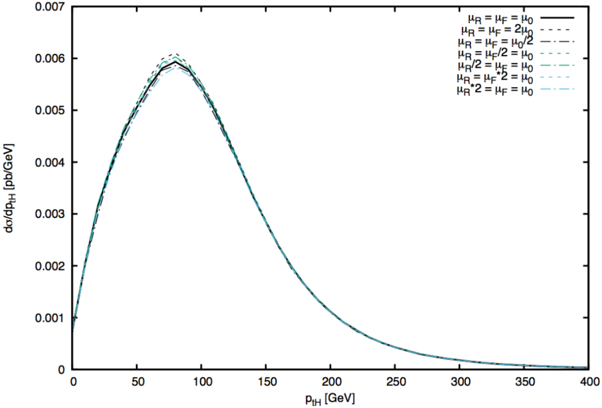

3- and 7-point scale variations are very close to eachother.

3-point vs 7-point scale variations

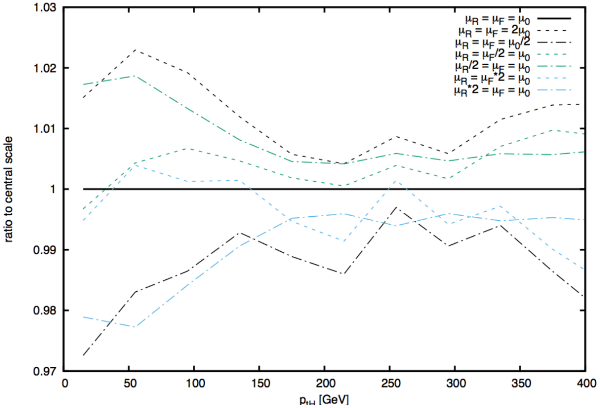

3- and 7-point scale variations are very close to eachother.

Choice of scale

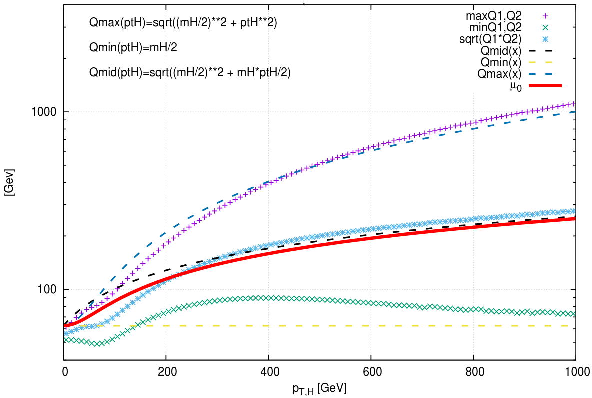

Our choice of $\mu_0^2(p_{t,H}) = \frac{M_H}{2}\sqrt{\left(\frac{M_H}{2}\right)^2 + p_{t,H}^2}$ is very close to a choice of $\mu = \sqrt{Q_1 Q_2}$.

VBF and Parton Shower

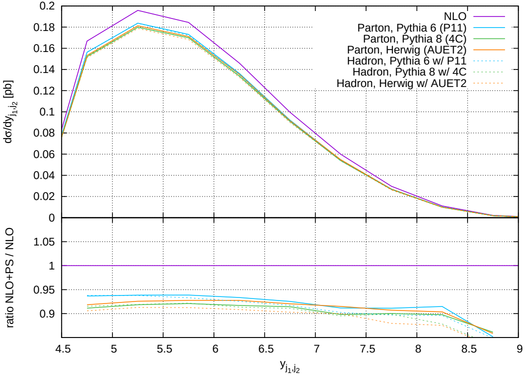

- different parton showers give relatively similar results
- hadronisation effects are consistently small

VBF Cuts

Due to huge QCD backgrounds a set of very selective cuts have to be applied. For this study we picked:

- jets defined with anti-k_t, $R = 0.4$ and $p_t > 25$ GeV
- two hardest jets within $|y| < 4.5$
- high dijet invariant mass, $M_{j_1 j_2} > 600$ GeV, and separation, $\Delta y_{j_1 j_2} > 4.5$
- hardest jets in opposite hemispheres, $y_{j_1} y_{j_2} < 0$

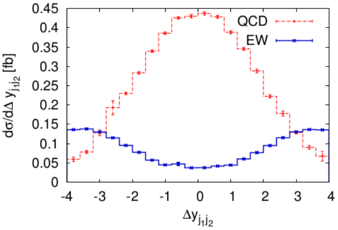

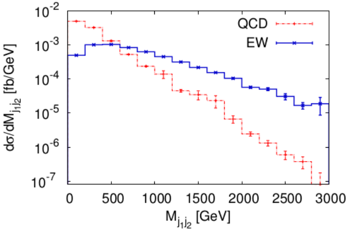

[Jäger, Zanderighi (2011)]

NNLO/NLO/LO PDFs

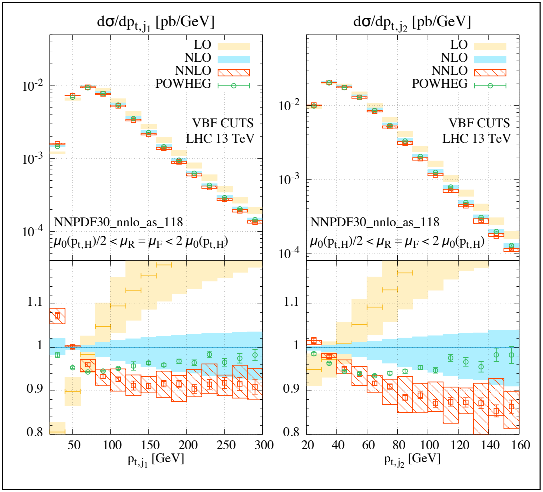

- LO results with LO PDFs
- NLO results with NLO PDFs
- NNLO results with NNLO PDFs

NNLO/NLO/LO PDFs

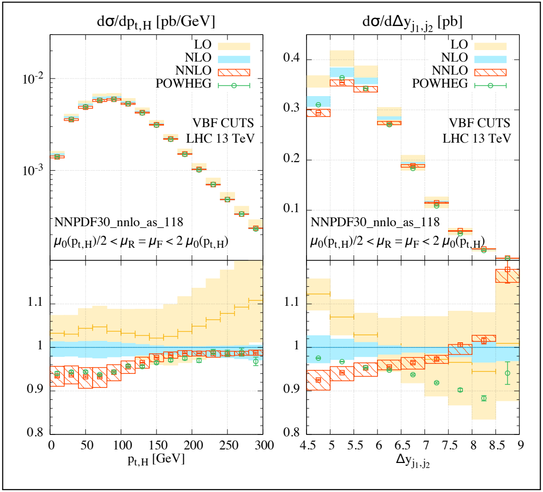

- LO results with LO PDFs
- NLO results with NLO PDFs
- NNLO results with NNLO PDFs